JOURNAL of
OSSEOINTEGRATION

> PATRICIA MIRANDA BURGOS[1], LUIZ MEIRELLES[1,2], LARS SENNERBY[1]

[1] Department of Biomaterials, Institute for Surgical Sciences, Sahlgrenska Academy at Gothenburg University (Sweden)
[2] Department of Prosthetic Dentistry, Institute of Odontology, Sahlgrenska Academy at Gothenburg University (Sweden)

Early bone formation in furrows at titanium implants. A study in the rabbit tibia

ABSTRACT

Aim Previous studies have shown a preference for bone formation in macroscopic furrows as compared to other parts of the implant surface. The aim of the study was to describe the early events of bone integration of furrowed oxidized titanium implants.
Materials and Methods New Zealand white rabbits and 54 implants were used in the study. The test oxidized implants had a 110 µm wide furrow added to the superior flank whilst the control oxidized implants had no furrow. The implants were retrieved after 7, 14 and 28 days for light microscopy and for micro-CT evaluation.
Results The bone contact and bone area values increased with time for all implants. A statistically significant preference for bone formation in the furrows was seen for test implants and for the inferior thread flank for control implants compared to the opposing superior thread flank. The 3D reconstructions from micro-CT showed bone formation as thin rims along the implant surface either continuous or as solitary rims.
Conclusion It is concluded, that bone formation is observed more often at the lower flank and in macroscopic furrows at the threads than opposing upper flanks of oxidized titanium implants. This was more marked at seven days than later time points and in areas with no primary contacts with adjacent host bone. Bone integration of the implants seemed to occur by bone condensation directly at and along the implant surface and following the path of the implant threads.

KEYWORDS Bone formation; Dental implants; Morphometric analysis; Surface modification.

INTRODUCTION

The tissue response to biomaterials after implantation in soft and bone tissues is influenced by nano-, micro- and macrotopography of the biomaterials surface (1, 2, 3). Such knowledge can be useful when designing new osseointegrated implants in order to optimize and possibly shorten the time for bone integration. With regard to surface topography, numerous studies have shown the formation of more direct bone contacts and have demonstrated higher stability when using pullout and removal torque tests (4-12). It is generally believed that surface modified implants results in better clinical outcomes and consequently most of the commercially available osseointegrated implants have a surface modified by plasma-coating, blasting, etching, anodic oxidation or combination of techniques (13). However, from a strict scientific point of view there is little support from the literature for such a conclusion (14).
Changes of the macrogeometry by adding furrows on the surface of a biomaterial can have an influence on cell orientation and migration by so called contact guidance (1). In two previous animal investigations using furrowed oxidized titanium implants, it was observed that newly formed bone tissue was more often found in furrows than at surfaces without a furrow (15, 16). Moreover, removal torque tests showed a significant improvement of stability for 110 µm wide furrows as compared with control implants with no furrows after 6 weeks of healing. This was observed neither for 80 µm nor for 200 µm wide furrows. Light microscopy of the bone-implant interface after removal torque testing revealed an increasing occurrence of fractures of the bone at the furrow entrance with decreasing width, while separation of the bone-implant interface was observed for control implants. It was suggested that

the increased stability was a result of an improved interlocking due to ingrowth of adjacent supporting bone rather than as a result of the observed bone affinity *per se* and that the 110 µm wide furrow for some unknown reason showed the highest peak removal torque (15, 16). However, the observed phenomenon as such calls for more studies investigating the early tissue responses to furrowed implants. It would be interesting to find out if the observed bone formation is a solitary event, for example due to constraining of cell populations, or if it is the result of guided bone growth from areas of primary bone contacts.

The aim of the present animal study was to histologically describe the early bone tissue responses to furrowed oxidized titanium implants. The purpose was also to use SEM and micro-CT techniques to study the spatial relation between the newly formed bone and the furrowed surfaces.

MATERIALS AND METHODS

Animals and anaesthesia

Nine female New Zealand white rabbits at least 8 months old were used in the study. The animals were kept free in a purpose-designed room and were fed *ad libitum* with water and standard laboratory animal diet and carrots. Prior to surgery, the animals were given general anaesthesia by an intramuscular injection of fluanison and fentanyl (Hypnorm, Janssen Pharmaceutica, Brussels, Belgium 0.2mg/kg and intraperitoneal injection of diazepam (Stesolid, Dumex, Copenhagen, Denmark) 1.5mg/kgbody weight. Additional Hypnorm was added when needed. Local anaesthesia was given using 1 ml of 2.0% lidocain/epinephrine solution (Astra AB, Södertälje, Sweden). After surgery the animals were kept in separate cages until healing of the wounds (1-2 weeks) and then released to the purpose-designed room until termination. Postoperatively, the animals were given antibiotics (Intenpencillin 2.250.000 IE/5 ml, 0.1 lm/kg body weight, LEO, Helsingborg, Sweden) and analgesics (Temgesic 0.05mg/kg, Reckitt and Colman, NJ, USA) as single intramuscular injections for three days. The study was approved by the local committee for animal research.

Implants

A total of 72 threaded titanium implants, 3.75 mm in diameter and 7 mm long (MKIII, Nobel Biocare AB, Gothenburg, Sweden) without any apical undercut features were inserted in the rabbits and three implant groups were selected. The test implants (n=27) had a single furrow, 70 µm deep and 110 µm wide, positioned at the center of the superior thread flank (Fig. 1). A second group of implants (n=27) without furrow were used as controls. The test and control implants were subjected to anodic oxidation (TiUnite, Nobel Biocare AB, Gothenburg, Sweden) which resulted in a porous surface structure as described elsewhere. A third group of implants (n=18) with turned surface and no furrows were also placed but the results will not be reported in this study. Both tibial metaphyses and the distal femoral condyles were used as implantation sites. The experimental areas were exposed via a skin incision medial to the knee-joint and separate incisions through fascia and periosteum above each site. Three holes were drilled in each tibial methaphysis and one in each femoral condyle using 1.8 mm, 2 mm and 3 mm twist drills during generous cooling by saline. No countersink drill was used.

Three implants, one from each group, were inserted in each tibial methaphysis. One test implant was inserted in one femoral condyle and one control implant in the contralateral side. Thus, each animal received a total of 8 implants. The fascia-periosteal flap and the skin were closed in separate layers with resorbable sutures. Three animals at a time were killed after 7, 14 and 28 days by an overdose of pentobarbital (Mebumal, ACO Läkemedel, Solna, Sweden).

Tissue processing and analyses

All implants and surrounding bone tissue were retrieved *en bloc* and fixed by immersion in 4% buffered formaldehyde. The implants from the left tibial methaphysis from each animal were used for micro-CT as described below; whereas the implants from the right tibial methaphysis were dehydrated in

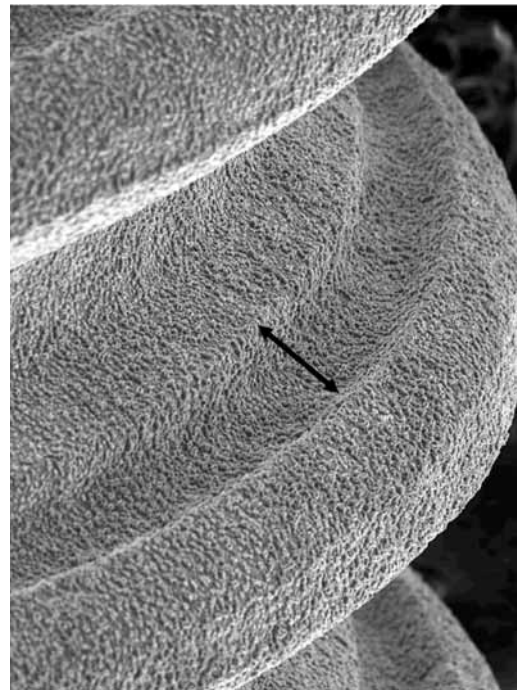

Fig. 1 *SEM of a test implant. Note the furrow at the upper thread flank.*

graded series of ethanol an embedded in light curing plastic resin, according to the method described by Donath (17). Sections were taken through the longitudinal axis of each implant by sawing and grinding (Exakt Apparatebau, Norderstedt, Germany). The sections, about 10 µm thick, were stained with toluidine blue and 1% pyronin-G. Examinations were performed in a Nikon Eclipse 80i microscope (Teknooptik AB, Huddinge, Sweden) equipped with an Easy Image 2000 system (Teknooptik AB, Huddinge, Sweden) using x1.8 to x100 objectives for descriptive evaluation and morphometrical measurements. The qualitative analysis aimed at describing the early bone formation events at the oxidized surface in general and in the furrows in particular. Of interest was also to study the sequence of bone fill in the furrows with time and with increased distance from the cortical bone.

The histometric evaluation comprised the following.

- Measurements of the degree of bone-implant contacts.
- Measurements of the bone area occupying the implant threads.
- Measurements of number of furrows with bone tissue in test implants.
- Measurements of the number of surfaces opposing the furrow showing bone formation.
- Measurements of the number of surfaces, corresponding to the position of the furrow in test implants, showing bone contact in control implants.
- Measurements of the number of surfaces opposing the corresponding furrow surface showing bone formation in control implants.

The implants from the left tibia were analysed with SkyScan 1172 micro-CT equipment (Micro Photonics Inc, Allentown, PA, USA). The desk-top X-ray microscanner consists of a microfocus sealed X-ray tube 20-100kV/0-250µA with 5µm spot size, a micro positioning stage (ideal to achieve exact positioning of small objects in the middle of the scanning field), an X-ray CCD-camera and an external computer with Dual Intel Xeon processors operated under Windows-XP Professional operation system. For microtomographical reconstruction transmission X-ray images are acquired from 200-3600 rotation views over 180 or 360 degrees of rotation. Both the X-ray tube and the camera operate under computer control. A software specifically designed for analyzing bone and similar structures were used which enable analysis of series of slices individually or as a 3D volume (CT-analysis, Micro Photonics Inc, Allentown, PA, USA). The technique allowed for virtual 3D reconstruction of each specimen which could be rotated and studied from different angles. In addition, bone tissue and titanium could be color marked due to differences in opacity. The path of bone in relation to the implant surface and its geometry could thus be studied.

Statistics

Descriptive data of measured parameters were used for the different time points. The Wilcoxon Rank Sign test was used on pooled data from 7,14 and 28 days and a difference considered if $p > 0.05$.

RESULTS

Light microscopy

A typical specimen comprised the implant which passed through a thin, about 1.5 mm, cortical layer and protruded into bone marrow tissue. Cancellous bone was present at one or both sides of all implants in femoral sites and in some specimens in the proximal tibia.

- Seven days: Light microscopy of 7 day specimens revealed bone debris from the drilling procedure and a re-organized loose connective tissue with large vessels at the tissue-implant interface. Non-bone areas consisted of a loose connective tissue rich of vessels, fat cells and haemopoietic cells. There were no signs of any inflammatory infiltrate although scattered inflammatory cells such as macrophages could be seen.

  Bone formation was seen to occur from the periosteal and endosteal surfaces as well as at and around the dislocated bone particles (Fig. 2). Specimens with cancellous bone had more primary

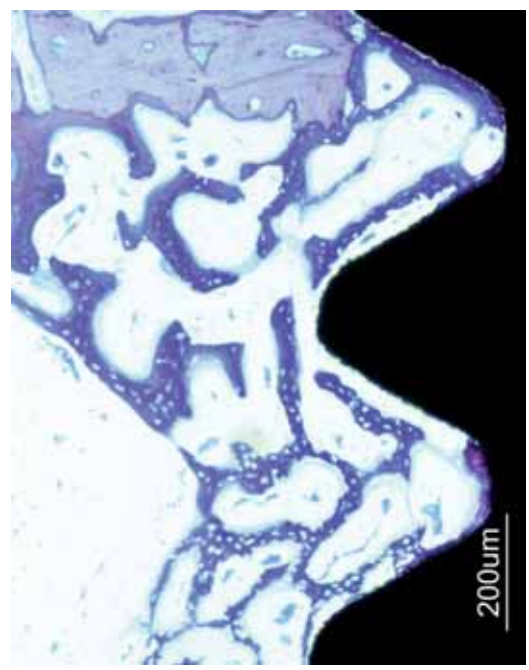

Fig. 2 *Light micrograph of a tibial specimen after 7 days: extensive formation of trabeculated bone towards a control implant. Toloudine blue.*

bone contacts with the implant and bone formation was seen on the surface of the bone trabeculae. Occasionally, bone from the endosteum and/or trabeculae reached the implant surface and bone formation extended over the implant surface. Solitary formation of woven bone was also seen in the bone marrow close to blood vessels but at a distance from existing bone and the implant surface. In these, scattered osteoblasts/osteocytes were surrounded by granular and globular aggregates.
Observation in high magnification revealed the presence of a darkly stained thin layer at the oxidized surface in various lengths, from solitary spots to continuous rims along several threads. This material had a globular appearance and seemed with few exceptions to be acellular (Fig. 3a). It filled the spaces between the surface irregularities. In addition, a lightly stained granular layer with numerous cells was seen on top of the dark layer (Fig. 3b). This was interpreted as osteoblasts producing bone matrix towards the underlying layer at the implant surface.

> Fourteen days: At 14 days more bone was contacting the implant. The bone rims at the implant surface were thicker and contained large randomly scattered lacunae with osteoblasts indicative of woven bone. The rims were usually lined with osteoid and osteoblasts indicating appositional bone formation towards the surroundings (Fig. 3b, 3c). A color difference could still be distinguished between the dark innermost interface layer and the lighter overlying bone tissue. Bone bridges interconnecting previously formed bone tissue, either at the surface, at existing bone surfaces or as solitary formations in the bone marrow were commonly seen. Extensive remodeling of the existing cortical bone was evident.

> Twenty-eight days: After 28 days, the bone had a more mature appearance due to extensive remodeling, i.e. replacement of the woven bone with lamellar bone. More bone was filling the implant threads. It was obvious that implants placed in cancellous bone had more bone at the interface due to bridging between bone trabeculae and the implant surface. The osteocyte lacunae were smaller than after 14 days. In bone marrow areas without existing cancellous bone, the newly formed bone at the implant surface did not fill the threads completely but followed the contour of the thread as a thin rim with a similar thickness as after 14 days, i.e. 50 to 150 um.

Morphometrical analyses

> Tibial implants: The morphometrical analyses revealed increasing bone contact and bone area values with time for both test and control implants in the tibia (Fig. 4a, 4b). At all time points the

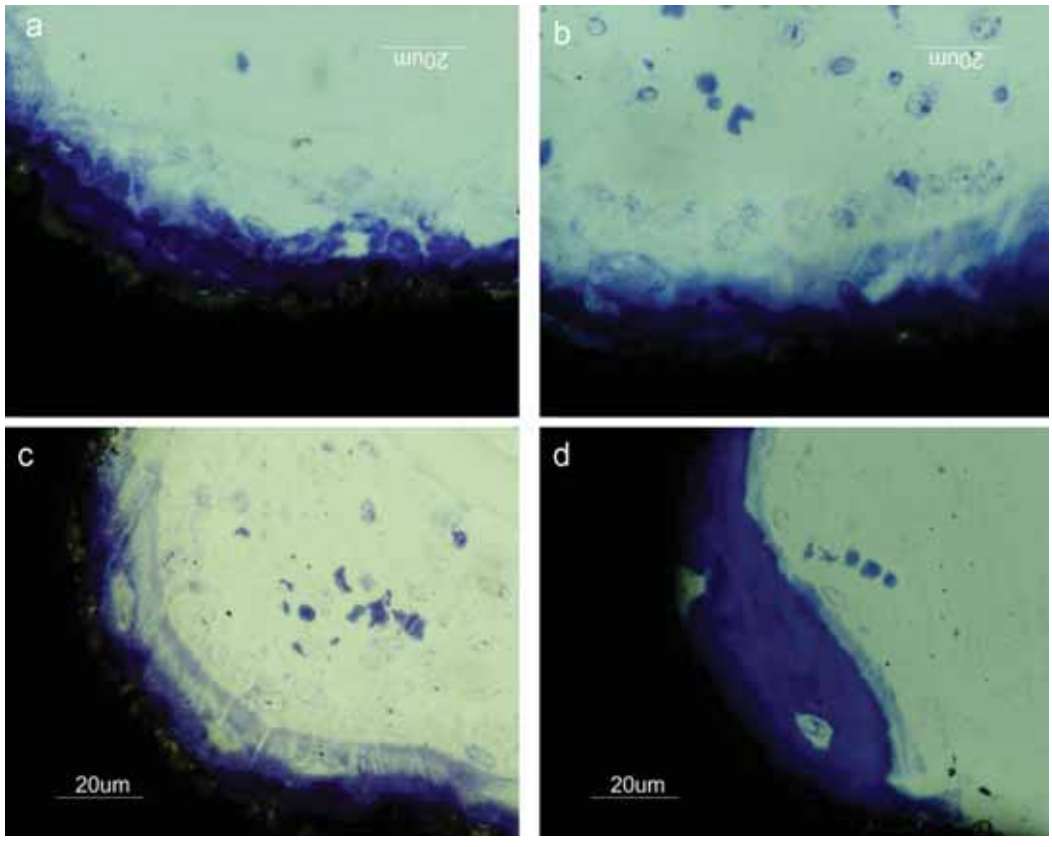

Fig. 3 *A series of light micrographs of furrowed implants showing formation of bone directly on the implant surface.*
a) A darkly stained layer about 10-15 µm thick with no or few cells can be observed. Osteoblasts and osteoid can be distinguished on top of this layer (7 days).
b) Osteoblasts are becoming entrapped in mineralized matrix (7 to 14 days).
c) Osteocytes can be seen in the interfacial bone layer. Active osteoblasts are seen to producing osteoid on the layer (7-14 days).
d)A thicker and more mature bone is observed after 28 days.

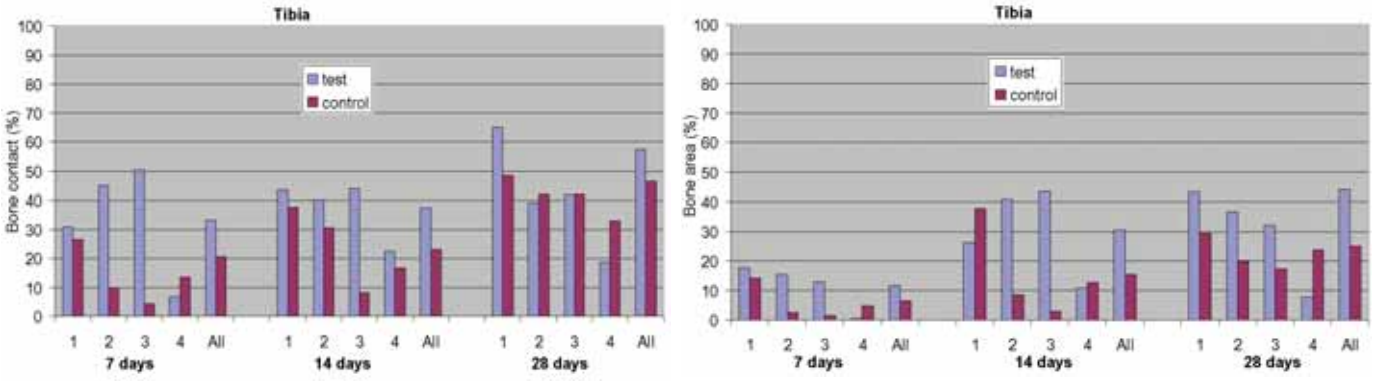

Fig. 4 *Graphs showing results from a/ bone-implant contact measurements and b/ bone area measurements for tibial implants.*

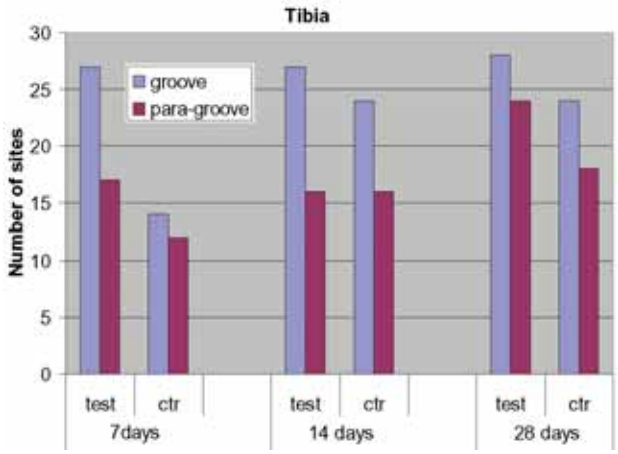

Fig. 5 *Graph showing results from calculations of number furrows with bone formation as compared with corresponding opposite thread flank without a furrow (para-furrow) for tibial implants.*

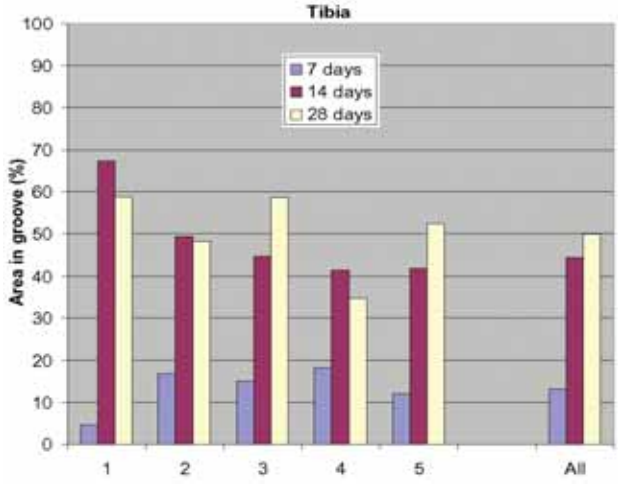

Fig. 6 *Graph showing results from bone area measurements in the furrows of test implants in the tibia.*

values were higher for test implants. However, no statistically significant differences were seen when pooling the data from the three time points. Control and test implants exhibited bone contact (%) of 29.5 + 23.0 and 39.3 + 21.7, respectively.

	Furrow	Para-furrow	Statistics
Test tibia	10 (0.9)	7 (2.7)	0.0147
Control tibia	7.3 (2.7)	4.8 (1.7)	0.0336
Test femur	9.4 (1.7)	6.8 (2.2)	0.0071
Control femur	8.6 (2.7)	7.6 (2.4)	0.0394

Table 1 *Pooled data from calculations of number of sites with bone formation in furrows vs opposing surface (para-furrow) for test implants and lower vs upper thread flanks for control implants. Wilcoxon Signed Rank test.*

Bone area (%) was 14.1 + 11.7 for control implants and 26.9 + 21.1 for test implants. Analysis of bone formation with thread level showed marked differences in threads 2 and 3 after 7 and 14 days, i.e. the threads located beneath the cortical layer. New bone formation was observed more often in furrows (lower flank) than at opposing surfaces (upper flank) for test implants and corresponding sites for control implants in tibial sites (Fig. 5). This was statistically verified when pooling data (Table 1). The difference was more marked after 7 than after 14 and 28 days. Also control implants showed a higher incidence of bone formation at lower than at upper thread flanks. Bone area measurements in the furrows showed an increased fill with time with a small difference between 14 and 28 days (Fig. 6). There was no particular pattern with regard to bone area and thread level.

> Femoral implants: Bone contact and bone area values for femoral implants increased with time and reached similar scores after 14 and 28 days (Fig. 7a, 7b). There were no or small differences between test and control implants at any time point when pooling the data. Control and test implants exhibited bone contact (%) of 46.9 + 19.4 and 47.3 + 22.1, respectively. Bone area (%) was 34.0 + 16.2 for control implants and 34.1 + 15.2 for test implants. Similar values were measured in all thread levels. Bone formation was evident more

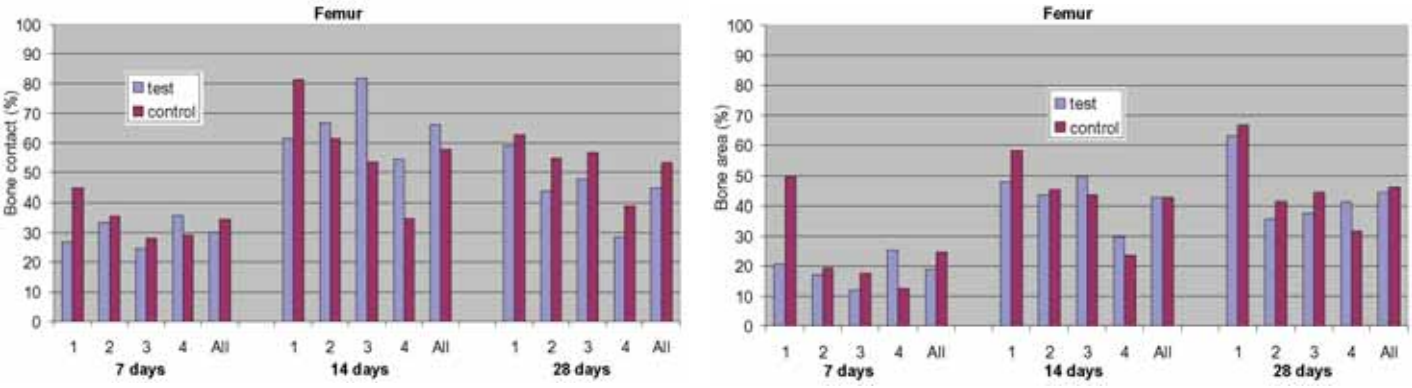

Fig. 7 *Graphs showing results from bone-implant contact measurements (a) and bone area measurements (b) for femural implants.*

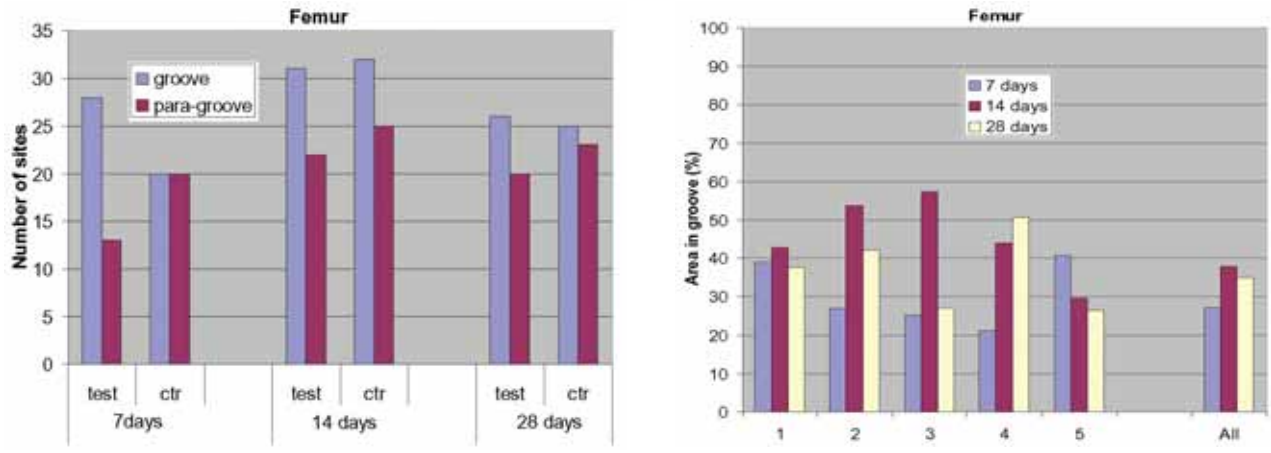

Fig. 8 *Graph showing results from calculations of number of furrows with bone formation as compared with corresponding opposite thread flank without a furrow (para-furrow) for femural implants.*

Fig. 9 *Graph showing results from bone area measurements in the furrows of test implants in the femur.*

often in furrows than at opposing surfaces at all time points (Fig. 8). The control implants showed no difference between upper and lower thread flanks after 7 days but a higher incidence of bone formation after 14 and 28 days. Pooled data showed statistically significant differences for both test and control implants in favor of the lower thread flank (Table 1). Bone area measurements in the furrows showed an increase from 7 to 14 days with no pattern with regard to thread level (Fig. 9).

Micro-CT

3D color-coded reconstructions revealed a pattern where new bone appeared to follow the path of the thread in apical direction for both test and control implants (Fig. 10). In addition, bone was observed to

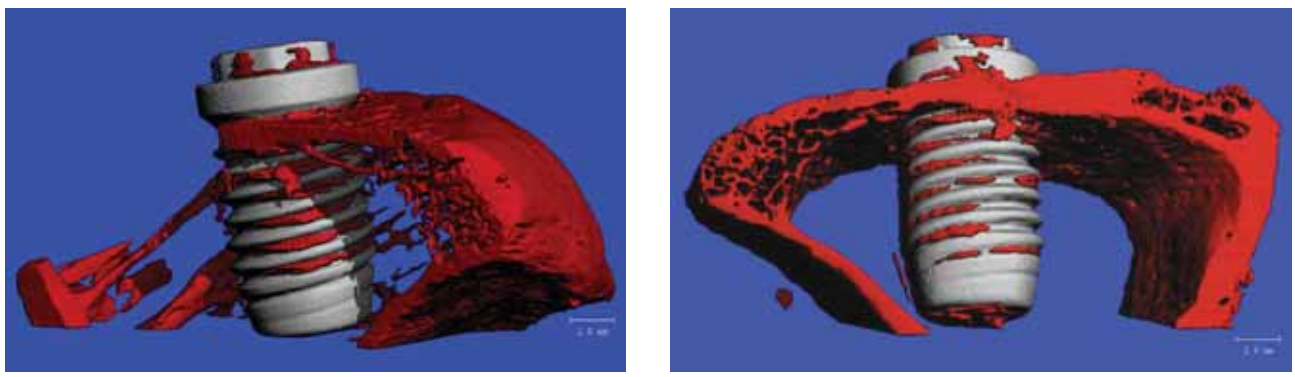

Fig. 10 *3D reconstruction of tibial implants test implant after 7 days (a) and control implant after 7 days (b).*

follow the path of the furrow (Fig. 11). The bone appeared as a continuation of existing bone in the marginal region as well as solitary rims. The sizes of the latter were from some hundreds micrometers to some millimeters. It was also evident that in cases of contact between existing bone and the implant surface, bone formation extended from that point. Solitary bone islands were never seen at the tip of the threads.

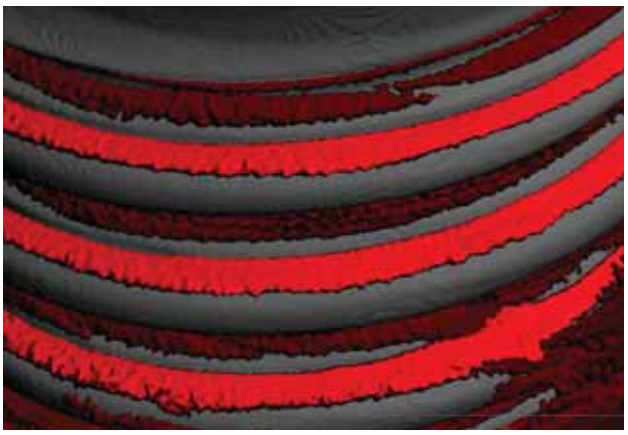

Fig. 11 *3D reconstruction of a tibial implant to demonstrate bone formation in the furrow after 14 days.*

DISCUSSION

The present animal study was conducted to analyze the early bone tissue response to furrowed oxidized titanium surfaces. Previous studies from our group have revealed an affinity to furrows located at one thread flank of such implants in comparison to the opposing thread flank (15, 16). Moreover, a correlation between decreasing furrow size and bone formation affinity was observed (16). In spite of this, a distinct increase of the resistance of removal torque was seen for 110 µm wide furrows as compared to widths of 80 and 160 µm and no furrows. This was the reason why 110 µm wide furrows were chosen in the present experiment.

The findings of the present study revealed bone formation directly at the implant surface for both tibial and femoral implasnts, which was more often observed in the furrows than at the corresponding site of the opposing flank for test implants in the tibia and the femur. A similar trend was, however, also seen for control implants which indicated that bone formation had an affinity to the inferior thread flank as such. The two observations could be statistically verified when pooling data from all three time points. This is in line with Larsson et al. (11), who observed a similar affinity of bone to the lower as opposed to the upper thread flank when evaluating titanium implants with four different surface topographies after 7 and 12 weeks of healing in the rabbit tibia. The overall bone contact and bone area values in the present study were higher for test implants in the tibia, although not statistically significant when pooling the data. Small or no differences were seen in femoral sites at any time point or when pooling the 7, 14 and 28 days data. This is probably related to the different morphologies of the peri-implant bone tissues at the two experimental sites. The tibia consists of a thin cortical layer and underlying bone marrow tissue, usually without any cancellous bone, while the femoral sites contain cancellous bone. Therefore, femoral implants had more primary contacts with bone from where bone formation at the implant surface could proceed. Bone formation was first seen as a darkly stained layer some 10 µm wide and filling the surface irregularities. No or few cells were seen in this layer. However, numerous cells often forming typical osteoblast and osteoid seams were seen at later stages of interfacial bone formation. The innermost dark layer could be distinguished also after 28 days, although much of the woven bone had been replaced with lamellar bone. The 3D reconstructions of tibia showed thin rims of bone at all time points following the contour of the threads, preferentially in the bottom of the threads and in the furrows. The findings indicated that bone formation started on the surface and proceeded in the direction towards the surrounding tissues and along the implant surface. Our findings corroborates with implant healing events as discussed by Davies and Hosseini (18). They suggested that the initial blood clot and its retention to the implant surface is an essential prerequisite for the migration of osteogenic cells. According to these authors, the bone forming process starts with *de novo* bone formation by newly differentiated osteogenic cells which form a cement line directly on the substrate surface. Such a line has previously been described to be some 500 nm up to 1 µm thick in a review on ultrastructural studies of the bone-implant interface (19). The limitations of the ground sectioning technique in combination with the irregular surface structures make it impossible to identify such thin layers. However, it is possible that the darkly stained layer observed in the present study corresponds to the layer described by Davies and Hosseini (18). Thereafter, bone conduction leads to bone formation along the implant surface in parallel with and increased thickness of the bone by appositional growth. Our histology confirms this version.

By using light- and transmission electron microscopy, Sennerby et al (20, 21) described the early tissue responses to turned titanium implants using the same rabbit model. In these studies, bone was formed as solitary islet in the matrix at a distance from the

implant surface and never directly at the surface. Instead, they described the presence of multinuclear cells which diminished with increased bone-implant contacts due to ingrowth of bone towards the surface. A cement line-like "lamina limitans" layer was also observed where bone contacts had been established. The observation by Sennerby et al and in the present study, suggest different pathways of implant integration. This has been previously described as contact and distance osteogenesis (22, 23)s. However, further comparative studies are needed to further investigate possible differences between bone formation at surface modified and turned titanium surfaces.

CONCLUSION

Bone formation occurs more often in macroscopic furrows at implant threads than opposing surfaces without a furrow. This was more marked at 7 days and in areas with no adjacent host bone. Bone integration of the implants seemed to occur by bone condensation directly at and along the implant surface and preferentially in the bottom of the threads and in the furrows.

ACKNOWLEDGEMENT

The study was supported by Nobel Biocare AB, Gothenburg, Sweden. Dr Peter Schüpbach and Mr Jan Hall are gratefully acknowledged for their assistance.

REFERENCES

1. *Brunette DM, Chehroudi B. The effects of the surface topography of micromachined titanium substrata on cell behavior in vitro and in vivo. J Biomech Eng. 1999;121:49-57.*
2. *Kieswetter K, Schwartz Z, Dean DD, Boyan BD. The role of implant surface characteristics in the healing of bone. Crit Rev Oral Biol Med. 1996;7:329-45. Review.*
3. *Meirelles L, Melin L, Peltola T, Kjellin P, Kangasniemi I, Currie, F, Andersson, M, Albrektsson T & Wennerberg A. Effect of hydroxyapatite and titania nanostructures on early in vivo bone response. Clin Implant Dent Relat Res. 2008;10:245-54.*
4. *Brunette DM. Principles of cell behaviour on titanium surfaces and their application to implanted devices. In Brunette DM, Tengval P, Textor M, Thomsen, P, eds. Titanium in medicine. Berlin: Springer; 2001:485-512.*
5. *Wennerberg A, Albrektsson T, Lausmaa J. Torque and histomorphometric evaluation of c.p. titanium screws blasted with 25- and 75-microns-sized particles of Al2O3. J Biomed Mater Res. 1996;30:251-60.*
6. *Ivanoff CJ, Widmark G, Johansson C, Wennerberg A. Histologic evaluation of bone response to oxidized and turned titanium micro-implants in human jawbone. Int J Oral Maxillofac Implants. 2003;18:341-8.*
7. *Ivanoff CJ, Hallgren C, Widmark G, Sennerby L, Wennerberg A. Histologic evaluation of the bone integration of TiO(2) blasted and turned titanium microimplants in humans. Clin Oral Implants Res. 2001;12:128-34.*
8. *Li D, Ferguson SJ, Beutler T et al. Biomechanical comparison of sandblasted and acid-etched and the machined and acid-etched titanium surface for dental implants. J Biomed Mater Res. 2002;60:325-32*
9. *Wennerberg A, Albrektsson T, Andersson B, Krol JJ. A histomorphometric and removal torque study of screw-shaped titanium implants with three different surface topographies. Clin Oral Implants Res. 1995;6:24-30.*
10. *Gotfredsen K, Berglundh T, Lindhe J. Anchorage of titanium implants with different surface characteristics: an experimental study in rabbits. Clin Implant Dent Relat Res. 2000;2:120-8.*
11. *Larsson C, Thomsen P, Lausmaa J, Rodahl M, Kasemo B, Ericson LE. Bone response to surface modified titanium implants: studies on electropolished implants with different oxide thicknesses and morphology. Biomaterials. 1994;15:1062-1074.*
12. *Meirelles L, Currie F, Jacobsson M, Albrektsson T, Wennerberg A. The effect of chemical and nanotopographical modifications on the early stages of osseointegration. Int J Oral Maxillofac Implants. 2008;23:641-47.*
13. *Cochran DL. A comparison of endosseous dental implant surfaces. J Periodontol. 1999; 70:1523-39.*
14. *Esposito M, Coulthard P, Thomsen P, Worthington HV. The role of implant surface modifications, shape and material on the success ofosseointegrated dental implants. A Cochrane systematic review.Eur J Prosthodont Restor Dent. 2005;13:15-31.*
15. *Hall J, Miranda-Burgos P, Sennerby L. Stimulation of directed bone growth at oxidized titanium implants by macroscopic grooves. An in vivo study. Clin Implant Dent Relat Res. 2005;(suppl):76-82*
16. *Miranda-Burgos P, Meirelles, L, Sennerby L. Influence of furrow width on affinity for bone formation and stability of grooved oxidized implants. A biomechanical and histological study in the rabbit. Submitted.*
17. *Donath K. Preparation of histologic sections by cutting–grinding technique for hard tissue and other materials not suitable to be sectioned by routine methods. Norderstedt: EXAKT-Kulzer-Publication; 1993. p.1–16.*
18. *Davies JE, Hosseini MM. Histodynamics of endosseous wound healing. In: Davies JE, ed. Bone engineering. Toronto: Em squared incorporated; 2000. p.1-14.*
19. *Albrektsson TO, Johansson CB, Sennerby L. Biological aspects of implant dentistry: osseointegration. Periodontol 2000. 1994;458-73.*
20. *Sennerby L, Thomsen P, Ericson LE. Early tissue response to titanium implants inserted in rabbit cortical bone. Part I Light microscopic observations. J Mat Sci Mat Med. 1993;4(3):240-250.*
21. *Sennerby L, Thomsen P, Ericson LE. Early tissue response to titanium implants inserted in rabbit cortical bone. Part II Ultrastructural observations. J Mater Sci Mater Med 1993;4(5):494-502.*
22. *Osborn JF, Newesely H. Dynamic aspects of the bone-implant interface. In: Heimke G, ed. Dental implants: materials and systems. Munchen: Carl Hansen Verlag; 1980. p.111-23*
23. *Davies JE. Understanding peri-implant endosseous healing. J Dent Educ. 2003;67:932-49*